$\mathcal{R}$esearch in
$\mathcal{A}$stronomy and
$\mathcal{A}$strophysics

# Galactic halo age estimated from LAMOST DR4 and *Gaia* DR1

Jin-Cheng Guo[1,2,3,*], Hua-Wei Zhang[1,2], Yang Huang[1,2,4,*], Xiao-Wei Liu[4,1,2], Ji-Feng Liu[3],
Mao-Sheng Xiang[3,*], Bing-Qiu Chen[4], Hai-Bo Yuan[5], Zhi-Jia Tian[1,2,*], Zhi-Ying Huo[3] and Chun Wang[1,2]

[1] Department of Astronomy, Peking University, Beijing 100871, China; *jincheng.guo@pku.edu.cn, zhanghw@pku.edu.cn*

[2] Kavli Institute for Astronomy and Astrophysics, Peking University, Beijing 100871, China

[3] Key Laboratory of Optical Astronomy, National Astronomical Observatories, Chinese Academy of Sciences, Beijing 100101, China

[4] South-Western Institute for Astronomy Research, Yunnan University, Kunming 650500, China

[5] Department of Astronomy, Beijing Normal University, Beijing 100875, China

**Abstract** The stellar halo is one of the major components in the Milky Way. Research on its age can provide critical constraints on the origin of the stellar halo and further on the formation of our Galaxy. So far, different approaches and samples have been used to estimate the age of the Galactic halo. In our previous paper, we carefully selected 63 field halo turn-off stars within 1 kpc from the literature using a kinematic approach, then estimated the age of the halo. In this following work, we not only update the data from LAMOST DR4 and *Gaia* DR1, but also try a different method to select a clean halo sample by combining the metallicity and orbital parameters. Then we compare this halo turn-off sample with the GARSTEC model in the $B - V$ vs. metallicity plane. After Monte Carlo simulations are performed, the age is estimated to be 10.5±1.4 Gyr, highly consistent with our previous result and other studies. However, due to the limited common sources between LAMOST DR4 and *Gaia* DR1, the final sample in this paper is still quite small. The estimated age will be more robust with the much larger *Gaia* DR2.

**Key words:** galaxies: halos — Galaxy: evolution — stars: kinematics and dynamics

## 1 INTRODUCTION

The stellar halo is one of the major components of the Milky Way, in addition to the Galactic bulge and disk. Despite this fact, the origin of the stellar halo is still unclear. There are two well established hypotheses regarding the formation of the halo. Eggen et al. (1962) declared that the Galactic halo was formed via rapid monolithic collapse, then Searle & Zinn (1978) claimed that it was formed from accretion of nearby satellite galaxies over several Gyr. Recently, Carollo et al. (2007) suggested that the Galactic halo is composed of inner and outer halos, which are two broadly overlapping structures. These two components show distinct density profiles, metallicities and stellar orbits. de Jong et al. (2010) pointed out that the inner halo dominates the inner part up to 10–15 kpc,

while beyond is the so called outer halo. Yet, this is challenged by Schönrich et al. (2011, 2014), who argued that this result is caused by systematic bias in estimation of distance. These debates make other parameters like age crucial to further understanding the origin and structure of the Galactic halo.

There are several methods to estimate the age of the stellar halo as a whole. One way is to use globular clusters as tracers to derive the age of the halo (Searle & Zinn 1978; Chaboyer et al. 1996; Sarajedini 1997; Guo et al. 2018). Another approach is to use the difference in color between the main sequence turn-off and the base of the red giant branch (Sarajedini & Demarque 1990; Vandenberg et al. 1990). The age estimated by this method is relatively more accurate. Other methods for estimation of the halo stars' age include measuring the abundances of radioactive species, i.e. thorium and uranium (Frebel et al. 2007).

---

Nevertheless, the precision of this approach is less than $\sim 2$ to $3\,\mathrm{Gyr}$. More recently, Kalirai (2012) adopted halo stars that have just turned into white dwarfs, and used their masses to determine the age of the halo through a relation between the mass and age. Finally, they estimated the inner halo age to be $11.4\pm0.7\,\mathrm{Gyr}$.

According to the stellar evolution model, theories can also predict the age for a given star in a color versus brightness diagram, based on the relationship between the age, temperature, composition, distance and luminosity. Holmberg et al. (2009) adopted this method to further estimate the age of the halo. Jofré & Weiss (2011) used a similar approach to determine the age. The main sequence turn-off sample was identified by metallicity information acquired from Sloan Digital Sky Survey (SDSS) Data Release 7 (DR7) halo stars. Finally, their age was obtained to be $10$–$12\,\mathrm{Gyr}$, which is consistent with the inner halo age estimated by Kalirai (2012). Our previous paper also used the field halo main sequence turn-off stars as a probe to determine the Galactic halo age (Guo et al. 2016). From the Set of Identifications, Measurements, and Bibliography for Astronomical Data (SIMBAD) archive, we selected the halo membership via a kinematic method rather than metallicity. Then the color-magnitude diagram of the turn-off halo stars was used to obtain the age.

In this work, we updated the research sample with common stars from Large Sky Area Multi-Object Fiber Spectroscopic Telescope (LAMOST) Data Release 4 (DR4) and the *Tycho-Gaia* Astrometric Solution (TGAS, Michalik et al. 2015). By constraining the metallicty, we first roughly identified the likely halo stars. Then, we used the color versus absolute magnitude diagram and isochrones to pick out the turn-off sample. Furthermore, we calculated the orbital parameters for each halo turn-off candidate, and combined with the eccentricity and metallicity to finally confirm the halo membership. By adopting the same technique, the age of the halo is determined. In Section 2, we present our sample selection. In Section 3, we describe the method to obtain the age of the halo using our selected halo turn-off stars. The discussion and conclusion are presented in Sections 4 and 5, respectively.

## 2 DATA

### 2.1 Data Selection

As a follow-up work of our previous study (Guo et al. 2016), one of the primary goals is to update the SIMBAD database with a more self-consistent and accurate database. Therefore, the sample was selected from the common

stars between LAMOST DR4 and TGAS. LAMOST DR4 contains $7\,681\,185$ spectra observed from October, 2011 to June, 2016. The fundamental parameters of LAMOST DR4 objects adopted here were derived by the LAMOST Stellar Parameter Pipeline at Peking University (LSP3, Xiang et al. 2015). *Gaia* released its first data compilation with a total of $1\,142\,679\,769$ sources (Gaia Collaboration et al. 2016). However, only $2\,057\,050$ sources include positions, parallaxes and proper motions, a collection which is called the TGAS catalog.

Since *Gaia* only published its first release, the measurements of positions, parallaxes and proper motions are not accurate enough for scientific research. Therefore, *Gaia* data were combined with the previous *Tycho*-2 Catalogue as additional information for a joint solution with early *Gaia* data, which was used to generate TGAS. There are a total of $4\,373\,824$ unique sources from LAMOST LSP3 DR4, and for TGAS, there are $2\,057\,050$ unique sources in total. However, due to the very bright magnitude range of TGAS (Fig. 1), there are only $248\,677$ unique common sources left, after cross matching LAMOST LSP3 DR4 with the TGAS catalog within $3''$. As the *Gaia* observations continue, much more data with fainter magnitude and more independent measurements will be released. Hence, this work will benefit from this most accurate and ambitious astrometric mission in years to come.
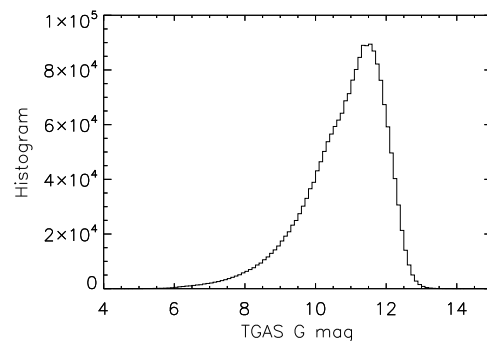


**Fig. 1** Histogram of G magnitude from TGAS. As this figure demonstrates, most TGAS sources are brighter than 12 magnitude.

### 2.2 The Turn-off Stars as Age Indicators

There are several ways to determine the age of the halo. In this work, we adopted the turn-off halo stars as age indicators. Generally, the position of the turn-off halo stars in the Hertzsprung-Russell (H-R) diagram will yield the age of the halo. Therefore, after correction for interstellar extinction in $B-V$ color, we first need to select turn-off stars

in the H-R diagram. Then, after further identification of reliable halo stars, the comparison of halo turn-off position and theoretical isochrones will reveal the age of the halo.

Among the ∼0.25 million common sources, we constrained the metallicity to be less than –1.0 and larger than –5.0, based on the metallicity distribution function in figure 7 from Ivezić et al. (2008), in order to roughly rule out the most likely disk stars. The effective temperature and signal to noise ratio (S/N) were also required to be less than 8000 K and greater than 15, respectively. Under these conditions, the accuracy of parameters derived from LSP3 is ensured. There are 1797 sources left after this selection process. For the purpose of obtaining self-consistent and accurate photometry, these sources were then cross matched with the AAVSO Photometric All-Sky Survey (APASS, Henden & Munari 2014). 1695 sources were found to be observed by APASS with $B$ and $V$ bands. 102 sources are left without APASS photometry, and 97 of them were found to have $B$ and $V$ band photometry from various literatures. We also acquired three-dimensional (3D) extinction data from 3D Dust Mapping with Pan-STARRS 1 (*http://argonaut.skymaps.info*; Green et al. 1987; Chambers et al. 2016). This extinction correction was adopted to correct the slight reddening in color index, therefore no systematic bias in determining the age will be introduced.

The likely halo sample was first plotted in the $B - V$ vs. absolute $V$ magnitude diagram (Fig. 2), which is similar to the H-R diagram, together with GARSTEC isochrones (the Garching Stellar Evolution Code, Weiss & Schlattl 2008). The absolute $V$ magnitude is derived from TGAS parallax and APASS apparent magnitude $V$. Then a rectangular region was defined to select turn-off stars illustrated by the magenta box in Figure 2. The region was defined to cover all the minimum values of $B - V$ for the GARSTEC evolution tracks at $Z = 0.0001$ and 0.001 within tolerance defined by measurement error, i.e. 0.05 mag and 0.1 mag in color index and absolute magnitude, respectively. This process is supposed to select most of the turn-off stars from the likely halo sample with very few contaminations. In the end, 110 turn-off stars are selected from the rectangular region after removal of one binary star according to SIMBAD.

## 2.3 Identification of the Halo Stars

### 2.3.1 Calculation of orbital parameters

According to the metallicity distribution function in Ivezić et al. (2008), stars with metallicity below –1.0 are more likely to be halo stars. However, thick disk star contamination is still a risk. Based on the fact that thick disk stars tend to have a more circular orbit compared to halo stars (Li & Zhao 2017), we decided to utilize the orbital parameters of each star to further rule out possible thick disk stars. The eccentricity of a star is defined as below

$$e = \frac{R_{\mathrm{apo}} - R_{\mathrm{peri}}}{R_{\mathrm{apo}} + R_{\mathrm{peri}}} \quad , \qquad (1)$$

where $R_{\mathrm{apo}}$ is the maximum Galactocentric distance a star can reach in its orbit, while $R_{\mathrm{peri}}$ is the minimum Galactocentric distance a star can reach. Assuming a Galactic potential used by Gardner & Flynn (2010), the orbits of the likely halo turn-off star sample were integrated, in order to calculate the eccentricities. In their model, the Milky Way is composed by a Plummer (1911) bulge and inner core, a Miyamoto & Nagai (1975) disk and a spherical logarithmic halo. The characteristic parameters can be found in table 1 of Gardner & Flynn (2010)'s paper.

### 2.3.2 Halo selection using orbital parameters

Once the orbital parameters were derived, we decided to combine the eccentricity with metallicity to safely remove possible thick disk star contaminants from the likely halo turn-off star sample. Based on the distribution in figure 7 of Ivezić et al. (2008), when the metallicity is below –1.5, there is almost no thick disk contribution. Therefore, we decided that for stars with metallicity below –1.5, no cut should be applied. But for stars with metallicity above −1.5, only those stars with eccentricity above 0.5 are considered as safe halo stars (Fig. 3). After the removal of 36 likely thick disk stars, there are 74 halo turn-off stars left in our sample. As Figure 3 demonstrates, we also consider the propagation error of eccentricity induced by the uncertainty of parallax and proper motions from TGAS. For the majority of stars with metallicity between –1.5 and –1.0 (e.g. black and red squares with error bars), the eccentricity derived from TGAS is accurate enough to be used to determine their thick disk or halo nature. However, for the remaining stars (blue crosses), their eccentricity with additional propagation error exceeds the eccentricity boundary of 0.5. Particularly, there are 11 stars classified as halo stars, even though their eccentricity may possibly be less than 0.5, after considering their propagation error. Therefore, we have re-checked the age determination procedure after the removal of these 11 stars. The re-estimated age is consistent with our initial result. Although we believe the choice of 0.5 as the eccentricity cut is suitable, it should be emphasized that this choice is a bit arbitrary.
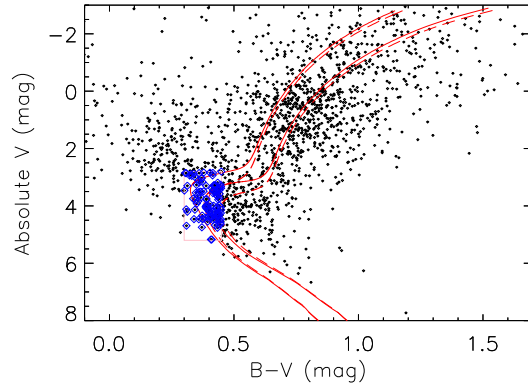
**Fig. 2** $B - V$ vs. absolute $V$ magnitude, similar to the H-R diagram. *Black dots* represent all likely halo stars selected by the metallicity cut. The overplotted left *red solid line* and *red dashed line* are the GARSTEC evolution tracks for isochrones of 10 Gyr and 14 Gyr at $Z = 0.0001$, respectively, while the *red solid line* and *red dashed line* on the right are tracks for isochrones of 10 Gyr and 14 Gyr at $Z = 0.001$, respectively. The *blue diamonds* inside the *magenta box* are defined as turn-off stars.
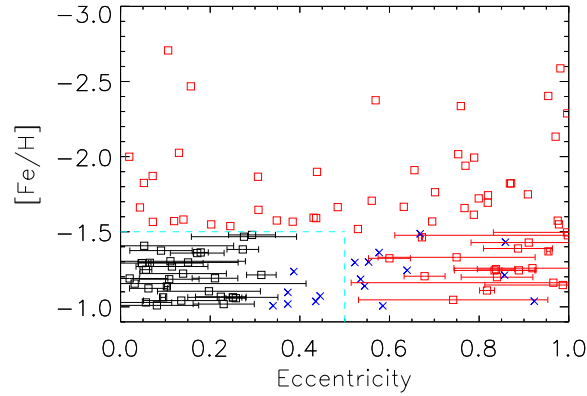


**Fig. 3**  This figure shows all likely halo turn-off stars in the orbital eccentricity vs. [Fe/H] space. *Red squares* without error bars represent the safe halo star population selected from the metallicity cut below –1.5, while *red squares* with error bars are orbital-parameter selected halo turn-off stars with a propagation error of eccentricity above 0.5. *Black squares* and *blue crosses* inside the *cyan box* are considered as thick disk stars based on their orbital parameters. Also, *blue crosses* in the *cyan box* are likely thick disk stars with a propagation error of eccentricity more than 0.5, and *blue crosses* outside the *cyan box* are likely halo stars with a propagation error of eccentricity less than 0.5.
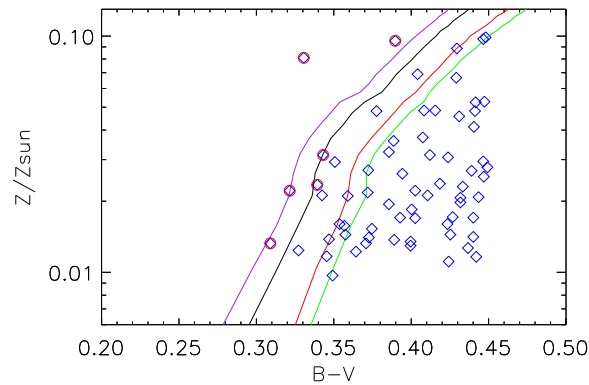


**Fig. 4**  $B - V$ vs. metallicity/solar plot. The turn-off halo star sample is overplotted with the GARSTEC isochrones at 9 Gyr, 10 Gyr, 12 Gyr and 13 Gyr. *Blue diamonds* are the final turn-off halo star sample, while *purple circles* are contaminations of the blue stragglers and binaries.

## 2.4 Blue Straggler Contamination

Since using the evolutionary population synthesis to study the properties of unresolved stellar populations should take the blue stragglers into account, Xin et al. (2007) suggest that the contamination of blue straggler stars in the main sequence turn-off sample selected from Galactic open clusters is about 10%. Similarly, the same contamination rate is assumed in this work. Thus, the bluest six sources, most likely to be blue stragglers, are removed (purple circles in Fig. 4). The remaining 67 stars (blue circles in Fig. 4) are finally used to estimate the age.

## 3 THE AGE OF THE HALO

Basically, the bluest $B - V$ of turn-off stars is related to a certain age and metallicity. Thus, the turn-off stars are plotted in the space of $B - V$ vs. metallicity ($Z$). The GARSTEC (Salaris et al. 2000) isochrones with atomic diffusion of 10 Gyr, 11 Gyr and 12 Gyr are also overplotted with the turn-off halo stars, as shown in Figure 4. The age of the halo is determined by the blue boundary of $B-V$ for turn-off halo stars. However, since there are only 67 turn-off halo stars in our sample, we adopted the same quantitative approach, as described in Guo et al. (2016), to determine the boundary accurately. Since the distance in $B - V$ between different isochrones is roughly the same under the same metallicity, we define the $B - V$ distance as the distance between a turn-off halo star and an isochrone under the same metallicity. Then the best estimated age of the halo can be expressed as

$$\min_{\text{dis}} |\Delta_{B-V}(Z \mid \text{age})| \quad , \tag{2}$$

where $\Delta_{B-V}(Z \mid \text{age})$ represents the distance between the $B - V$ boundary of turn-off stars and the isochrone with age at metallicity $Z$. The minimum distance with a certain isochrone corresponds to the best estimated age.

Practically, the estimation of the halo age is affected by the uncertainty of $B - V$ and other contaminations in the halo turn-off star sample. Therefore, the boundary of the $B - V$ color index is rather blurred instead of displaying a clear trend. So, we introduced the Gauss-Hermite (G-H) function to fit the distribution of $B - V$ distance with a given age, in order to determine the blue boundary position. The G-H function is expressed as below

$$f(x) = \frac{1}{\sqrt{2\pi}\sigma} e^{-\frac{(x-\mu)^2}{2\sigma^2}} \times \left[1 + \frac{h_3}{\sqrt{3}}(2x^3 - 3x) \right. $$
$$\left. + \frac{h_4}{2\sqrt{6}}(4x^4 - 12x^2 + 3)\right], \tag{3}$$

where $x$ represents $\Delta_{B-V}(Z|\text{age})$ for all $Z$ and a given age, $\sigma$ is the standard deviation of the G-H function, $\mu$ is the mean, and $h_3$ and $h_4$ are the coefficients of the 3rd and 4th order Hermite polynomials, respectively. Considering that the derivative of the G-H function can be analytically derived, it is adopted in this work. In addition, the peak of the derivative of the G-H function is regarded as the boundary of the $B - V$ distance.

In order to determine the age of the halo and take the uncertainty of the photometry into account, we designed a Monte Carlo simulation. The $B - V$ errors are also from APASS and have a mean value of 0.02 mag. Then only the isochrones with fixed ages of 10.0, 10.5, 11.0, 11.5 and 12.0 Gyr are used. For each isochrone, random errors are added to the 67 turn-off stars. Each random error is randomly selected from a Gaussian distribution with its $B-V$ as the mean and corresponding $B-V$ error as the standard deviation. Then the minimum $B - V$ distance is derived from the peak of the derivative of the best fit G-H function. One of the simulations is illustrated in Figure 5. The entire simulation consists of one hundred repeated runs for each isochrone. After this, the mean value and standard deviation of the minimum boundary of $B - V$ distance from the simulated data are derived.

In the end, after the simulations have been run for all the isochrones, the age of the isochrone with the smallest $B - V$ distance corresponds to the age of the halo. In this work, the isochrone with the smallest $B - V$ distance turns out to be the one corresponding to 10.5 Gyr as well. Furthermore, after 100 simulations, the distribution of the boundary of $B - V$ can be fitted by a Gaussian profile (Fig. 6). The standard deviation of the distribution for an isochrone of 10.5 Gyr is 0.021 mag. Given that the mean $B - V$ difference between 10 Gyr and 12 Gyr is about 0.03 mag, the dispersion of the age re-scaled from 0.021 mag is derived to be 1.4 Gyr. Hence, the age of the Galactic halo estimated in this work is 10.5±1.4 Gyr.

## 4 DISCUSSION

In this paper, the age of the Galactic halo is estimated. The age is measured with metallicity and orbital parameter-selected field halo turn-off stars by comparing their color and metallicity with isochrones from the theoretical model. Unlike Jofré & Weiss (2011) and our previous work, the halo stars are first roughly selected according to metallicity, then combined with orbital parameters of each star, and rechecked in a Toomre diagram as well. It is more likely that this sample is cleaner than those two works in selecting halo stars, thanks to accurate measurements from
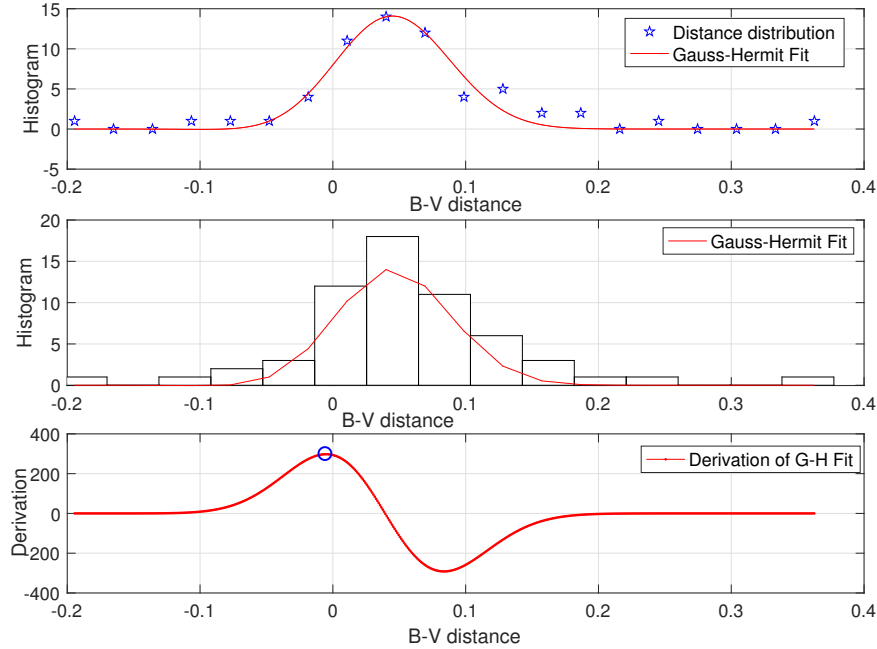
**Fig. 5** This figure is an illustration of one Monte Carlo simulation for an isochrone at 10.5 Gyr. $B - V$ distance is the distance between the isochrone and the star. Top and middle panels demonstrate the distance distribution and G-H fit of the distribution, while the bottom panel shows the derivative curve of the best fit G-H profile. The blue circle represents the maximum value of the derivative, indicating the boundary of turn-off stars.
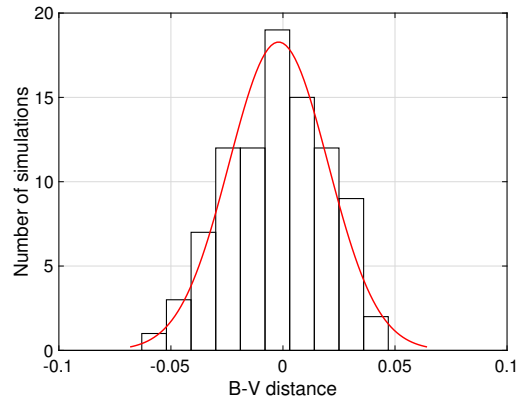


**Fig. 6** Distribution of the boundary of $B - V$ distance to the isochrone for 10.5 Gyr after 100 Monte Carlo simulations.

TGAS. According to figure 4 in Guo et al. (2016), there are still some stars with metallicity above −1.0 in the halo star sample of the previous work. Even though this does not affect the result by removing those stars, it still may not be a clean halo star sample. For Jofré & Weiss (2011)'s work, only applying the metallicity cut at −1.0 is also not enough. Compared to this work, with the accurate parallax and proper motion measurements from TGAS, reliable orbital parameters can be obtained to further rule out the contamination from thick disk stars. In addition, the age obtained in Jofré & Weiss (2011) is based on temperature and metal-

licity. The temperature is somehow model dependent, since it is derived from spectral fitting with atmosphere models. However, we determined the age based on $B - V$ color and metallicity. The photometric measurements are intrinsically more accurate. Our derived age of $10.5\pm1.4$ Gyr is the same as our previous work, and consistent with Jofré & Weiss (2011)'s result (10–12 Gyr), despite the different approaches and database we used. Our result is also in agreement with Kalirai (2012)'s result, which is $11.4\pm0.7$ Gyr and this age is estimated using white dwarfs.

The uncertainty of our result is still quite large compared with previous works. The first and most obvious reason is that the sample size is too small, owing to the limited size and very bright magnitude of TGAS data. As Figure 1 has shown, the majority of TGAS stars is brighter than 12 mag. Therefore, a huge number of these stars should be disk stars. Indeed, a large proportion of common stars between LAMOST and TGAS has been removed, since they are classified as disk stars using our selection method. Only 67 turn-off halo stars are left in the end to determine the age. For the purpose of increasing our halo sample, we have considered only adopting the LAMOST data, yet the accuracy of distance and proper motions from the pre-*Gaia* era is not comparable with the *Gaia* data. The uncertainty of age estimation is expected to be significantly reduced if the sample size could be much larger. Thus, the release of *Gaia* DR2 will definitely improve our result. Secondly, even though the extinction correction used in this work is uniform and slightly more reliable than the extinction used in Guo et al. (2016), uncertainty in the photometry could still be affected by the extinction correction. Thirdly, the contaminations from a selection of turn-off stars should also be noticed. Contaminations like binaries, blue stragglers, pulsators and so on may blur the boundary of turn-off stars. Last, mounting evidences have demonstrated that the halo is indeed composed of an inner halo and an outer halo (Searle & Zinn 1978; Carollo et al. 2007; de Jong et al. 2010; Beers et al. 2012; Das & Binney 2016). Owing to the different formation histories, the ages of the inner halo and outer halo vary. Therefore, the age of the halo should intrinsically form a dispersed distribution, rather than a fixed value. With the forthcoming release of *Gaia* DR2 and LAMOST DR5, we may have a unique opportunity to reveal the halo formation history by studying the age of the halo.

## 5 CONCLUSIONS

In this work, we estimated the age of the Milky Way halo by selecting turn-off halo field stars. Differing from our previous work, this time we select the halo stars using metallicity information combined with orbital parameters. Furthermore, this approach does not need to constrain the halo sample in the solar neighborhood, which is more suitable for finding more distant halo stars in large surveys like LAMOST and *Gaia*. However, there are only 67 turn-off halo stars left in the final age estimation, since the distance and proper motions in *Gaia* DR1 are only accurate enough at the very bright end. On the other hand, by adopting the GARSTEC model, which has considered atomic diffusion,

the observed data can match the theoretical stellar model without significant systematic bias in age determination. In addition, the estimated age and its error have taken the uncertainty of photometry and interstellar reddening into account. In the end, the age is derived to be $10.5 \pm 1.4$ Gyr, highly consistent with our previous result. This result is also in good agreement with Salaris & Weiss (2002), Jofré & Weiss (2011) and Kalirai (2012).

Obviously, some improvements could be made in the near future. With the release of *Gaia* DR2, a larger sample with fainter magnitude and improved accuracy in measurements can be established. Then combined with metallicity and other information obtained from LAMOST (Cui et al. 2012) and SDSS (York et al. 2000), a much larger halo turn-off sample will be constructed. The increase in the number of turn-off halo stars will definitely improve the reliability of our research and may aid us in testing the different formation histories of the long claimed inner and outer halos. On the other hand, the theoretical isochrone model used in this work could be tested and updated with newly developed models. For instance, MESA Isochrones & Stellar Tracks (MIST) is a relatively newly developed model based on MESA. It provides a large grid of single-star stellar evolutionary models extending across all evolutionary phases for all relevant masses and metallicities (Dotter 2016).

# References

Beers, T. C., Carollo, D., Ivezić, Ž., et al. 2012, ApJ, 746, 34

Carollo, D., Beers, T. C., Lee, Y. S., et al. 2007, Nature, 450, 1020

Chaboyer, B., Demarque, P., & Sarajedini, A. 1996, ApJ, 459, 558

Chambers, K. C., Magnier, E. A., Metcalfe, N., et al. 2016, arXiv:1612.05560

Cui, X.-Q., Zhao, Y.-H., Chu, Y.-Q., et al. 2012, RAA (Research in Astronomy and Astrophysics), 12, 1197

Das, P., & Binney, J. 2016, MNRAS, 460, 1725

de Jong, J. T. A., Yanny, B., Rix, H.-W., et al. 2010, ApJ, 714, 663

Dotter, A. 2016, ApJS, 222, 8

Eggen, O. J., Lynden-Bell, D., & Sandage, A. R. 1962, ApJ, 136, 748

Frebel, A., Christlieb, N., Norris, J. E., et al. 2007, ApJ, 660, L117

Gaia Collaboration, Brown, A. G. A., Vallenari, A., et al. 2016, A&A, 595, A2

Gardner, E., & Flynn, C. 2010, MNRAS, 405, 545

Green, E. M., Demarque, P., & King, C. R. 1987, The Revised Yale Isochrones and Luminosity Functions (New Haven: Yale Observatory)

Guo, J.-C., Liu, C., & Liu, J.-F. 2016, RAA (Research in Astronomy and Astrophysics), 16, 44

Guo, J.-C., Zhang, H. W., Zhang H. H., et al. 2018, RAA (Research in Astronomy and Astrophysics), 18, 32

Henden, A., & Munari, U. 2014, Contributions of the Astronomical Observatory Skalnate Pleso, 43, 518

Holmberg, J., Nordström, B., & Andersen, J. 2009, A&A, 501, 941

Ivezić, Ž., Sesar, B., Jurić, M., et al. 2008, ApJ, 684, 287

Jofré, P., & Weiss, A. 2011, A&A, 533, A59

Kalirai, J. S. 2012, Nature, 486, 90

Li, C., & Zhao, G. 2017, ApJ, 850, 25

Michalik, D., Lindegren, L., & Hobbs, D. 2015, A&A, 574, A115

Miyamoto, M., & Nagai, R. 1975, PASJ, 27, 533

Plummer, H. C. 1911, MNRAS, 71, 460

Salaris, M., Groenewegen, M. A. T., & Weiss, A. 2000, A&A, 355, 299

Salaris, M., & Weiss, A. 2002, A&A, 388, 492

Sarajedini, A. 1997, AJ, 113, 682

Sarajedini, A., & Demarque, P. 1990, ApJ, 365, 219

Schönrich, R., Asplund, M., & Casagrande, L. 2011, MNRAS, 415, 3807

Schönrich, R., Asplund, M., & Casagrande, L. 2014, ApJ, 786, 7

Searle, L., & Zinn, R. 1978, ApJ, 225, 357

Vandenberg, D. A., Bolte, M., & Stetson, P. B. 1990, AJ, 100, 445

Weiss, A., & Schlattl, H. 2008, Ap&SS, 316, 99

Xiang, M. S., Liu, X. W., Yuan, H. B., et al. 2015, MNRAS, 448, 822

Xin, Y., Deng, L., & Han, Z. W. 2007, ApJ, 660, 319

York, D. G., Adelman, J., Anderson, Jr., J. E., et al. 2000, AJ, 120, 1579